

Chapter 7

Weak interactions

As already discussed, weak interactions are responsible for many processes which involve the transformation of particles from one type to another. Weak interactions cause nuclear beta decay, as well as the decays of muons, charged pions, kaons, and many other hadrons. All processes which involve production or scattering of neutrinos, the conversion of quarks from one flavor to another, or the conversion of leptons from one type to another, involve weak interactions.

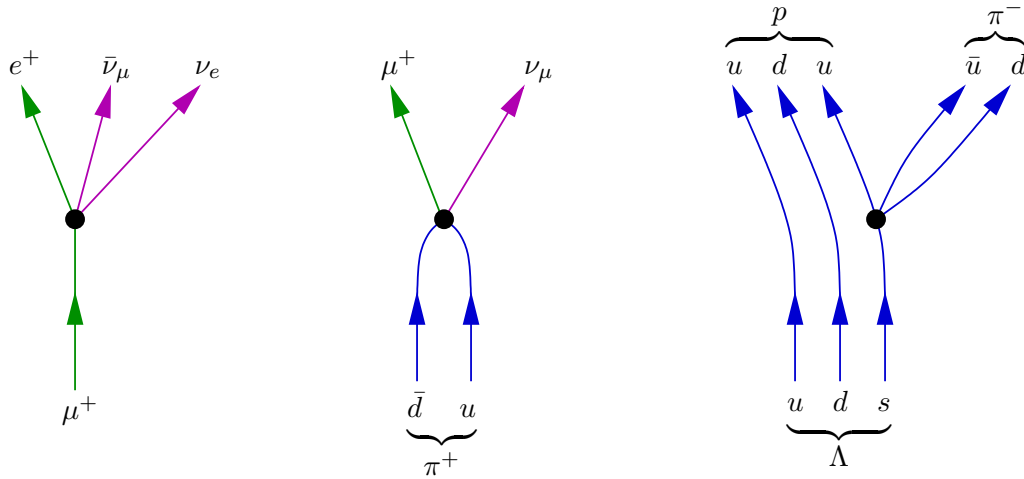


Figure 7.1: Depictions, at the level of quarks and leptons, of the weak decays $\mu^+ \rightarrow e^+ + \bar{\nu}_\mu + \nu_e$, $\pi^+ \rightarrow \mu^+ + \nu_\mu$, and $\Lambda \rightarrow p + \pi^-$.

Figures 7.1 and 7.2 depict, at the level of quarks and leptons, some of these weak interaction processes. As these figures illustrate, every weak interaction vertex (the black dot in the figures) involves four fermions (where here we are counting fermions and antifermions equally), either one fermion turning into three (as in muon decay) or two incoming fermions scattering and producing two outgoing fermions (as in neutrino scattering in Fig. 7.2). As the Λ baryon decay in Fig. 7.1 illustrates, there can also be *spectator* quarks which are constituents of the hadrons involved but not direct participants in the weak interaction process.

The complete Hamiltonian which describes particle interactions can be written as a sum of contributions from strong, electromagnetic, and weak interactions,

$$H = H_{\text{strong}} + H_{\text{EM}} + H_{\text{weak}} . \quad (7.0.1)$$

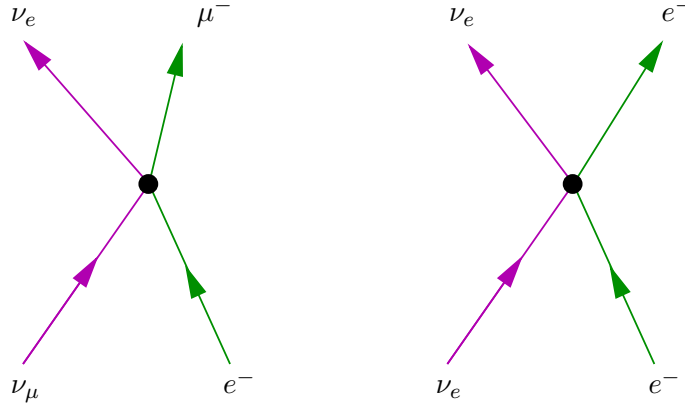


Figure 7.2: Left: inelastic neutrino scattering, $\nu_\mu + e^- \rightarrow \nu_e + \mu^-$. Right: elastic neutrino scattering, $\nu_e + e^- \rightarrow \nu_e + e^-$.

Because weak interactions are truly weaker than strong or electromagnetic interactions, it is useful to think of H_{weak} as a small perturbation to the dynamics generated by strong and electromagnetic interactions.

7.1 Muon decay

Consider (anti)muon decay, $\mu^+ \rightarrow e^+ + \bar{\nu}_\mu + \nu_e$, in Fig. 7.1. Let the ket $|\mu^+(\vec{p}=0)\rangle$ denote an initial state containing a single μ^+ at rest. Let the bra $\langle e^+(\vec{p}_e) \bar{\nu}_\mu(\vec{p}_{\bar{\nu}}) \nu_e(\vec{p}_\nu) |$ denote a final state describing a positron with spatial momentum \vec{p}_e , a muon antineutrino with momentum $\vec{p}_{\bar{\nu}}$, and an electron neutrino with momentum \vec{p}_ν . The existence of muon decay means that the time evolution of the initial state $|\mu^+(\vec{p}=0)\rangle$ will have a non-zero projection onto the final state $\langle e^+(\vec{p}_e) \bar{\nu}_\mu(\vec{p}_{\bar{\nu}}) \nu_e(\vec{p}_\nu) |$. This can only happen if the Hamiltonian, which generates time evolution, has a non-zero matrix element connecting these states. And this can only be due to the weak interaction part of the Hamiltonian. In other words, the existence of muon decay implies that the amplitude

$$M \equiv \langle e^+(\vec{p}_e) \bar{\nu}_\mu(\vec{p}_{\bar{\nu}}) \nu_e(\vec{p}_\nu) | H_{\text{weak}} | \mu^+(\vec{p}=0) \rangle, \quad (7.1.1)$$

is non-zero. The rate of decay must be proportional to the *square* of this amplitude. Because there are many different final states corresponding to different values of the final momenta p_e , $p_{\bar{\nu}}$ and p_ν , the complete decay rate Γ will involve a sum over all possible final states. Schematically,

$$\Gamma \sim \sum_{\text{final states}} |M|^2. \quad (7.1.2)$$

The amplitude M , when properly defined (see footnote below), will include momentum conservation, *i.e.*, the constraint that $\vec{p}_e + \vec{p}_{\bar{\nu}} + \vec{p}_\nu = 0$. When momentum is conserved, $p_{\bar{\nu}}$ will equal $-(p_\nu + p_e)$, so M may be regarded as function of two independent momenta, p_e and p_ν . This amplitude can, in principle, depend in some complicated fashion on these two final momenta. But the simplest possibility is for the amplitude to have minimal dependence on the outgoing momenta. Physically, this corresponds to a point-like interaction, for which the spatial variation of wavefunctions (due to their momentum) plays no role.

This approximation (that the weak interaction occurs essentially at a point) turns out to work remarkably well, and we will shortly discuss how we can understand this perhaps surprising result. If the amplitude M is momentum independent then, with just a little calculation, one can perform the sum over final states in Eq. (7.1.2) (strictly speaking, the 3-momenta are *continuous* variables and the sum is really an integral) and predict the muon decay spectrum as a function of either the positron energy or momentum. The spectrum is the fraction of decays in which the positron has energy between E and $E + dE$, or momentum between p and $p + dp$ with $E = \sqrt{p^2 + m_e^2}$. Figure 7.3 shows the comparison between experimental data for the decay spectrum versus momentum and the result of this calculation. The agreement is excellent.

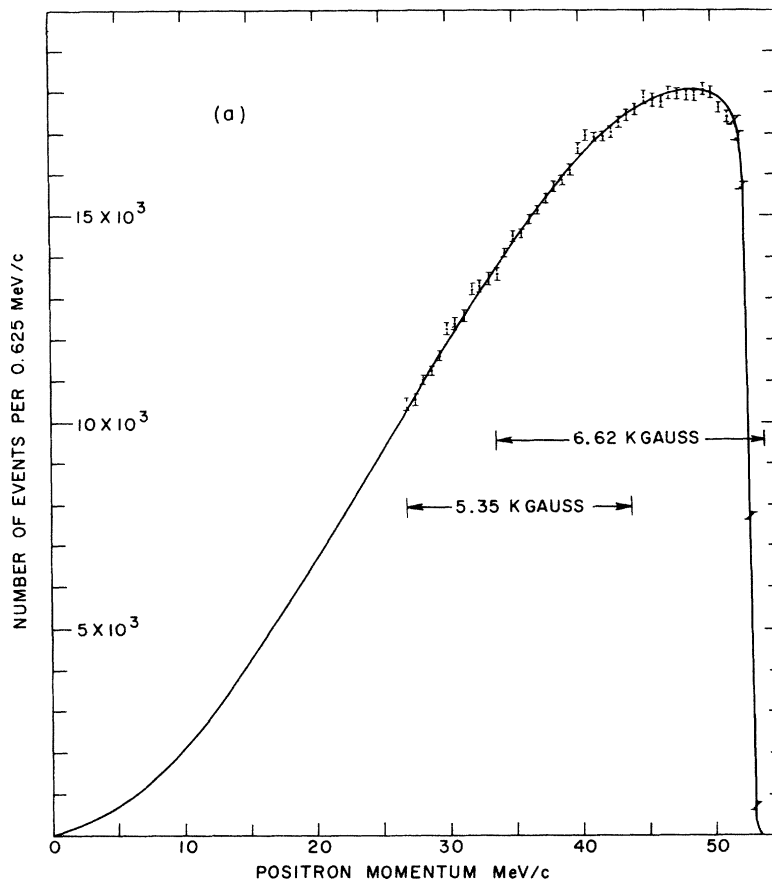


Figure 7.3: Energy spectrum of positrons emitted from decays of positively charged muons. The solid curve is the theoretical prediction; data points are shown with error bars. [From M. Bardon *et al.*, Phys. Rev. Lett. 14, 449 (1965)].

To characterize the value of the amplitude M , it will be useful to begin with some dimensional analysis. To make this as easy as possible, it will be convenient to use “natural units” in which $\hbar = c = 1$ (recall the discussion in section 2.7). Since c has ordinary dimensions of [length/time], setting $c = 1$ means that we are regarding length and time as having the same dimensions. Since \hbar has dimensions of [energy \times time], setting $\hbar = 1$ means that we are regarding energy and frequency (or inverse time) as having the same dimensions. Setting both \hbar and c to unity means that we are treating length and inverse energy as dimensionally equivalent. After using natural units in any

calculation, one can always reinsert factors of \hbar and c as needed to restore conventional dimensions. In particular, the value $\hbar c \simeq 197 \text{ MeV fm}$ may be regarded as a conversion factor which allows one to convert lengths measured in femtometers into lengths measured in MeV^{-1} , $1 \text{ fm} = \frac{1}{197} \text{ MeV}^{-1}$.

The Hamiltonian is the operator which measures energy. Its eigenvalues are the energies of stationary states. Therefore, the Hamiltonian must have dimensions of energy. If $|\Psi\rangle$ is any physical, normalized state, then the matrix element $\langle\Psi|H|\Psi\rangle$ is the expectation value of the energy in state $|\Psi\rangle$. Hence, matrix elements of the Hamiltonian, such as the muon decay amplitude M in Eq. (7.1.1), also have dimensions of energy, provided the states appearing in the matrix element are appropriately normalized as we will now discuss.

The wavefunction describing a particle with definite momentum \vec{p} is proportional to the plane wave $e^{i\vec{p}\cdot\vec{x}/\hbar}$. To normalize such a state, it is convenient to imagine that space is not infinite, but rather is limited to some finite, but arbitrarily large region \mathcal{V} . The condition that a state is normalized then becomes $1 = \int_{\mathcal{V}} d^3x |\Psi(\vec{x})|^2$, where the integral only includes the interior of the region \mathcal{V} . For simplicity, suppose that this region is a cube whose edges have length L (and hence volume L^3). A normalized state describing a particle with momentum \vec{p} will thus have a wavefunction $\Psi(\vec{x}) = e^{i\vec{p}\cdot\vec{x}/\hbar}/L^{3/2}$. The *absolute square* of this wavefunction gives a constant probability density of $1/L^3$ whose volume integral over the region \mathcal{V} equals one, as desired.

Now consider the muon decay amplitude M . The initial muon, with zero spatial momentum, will have a *constant* wavefunction, $\psi_{\mu}(\vec{x}) = 1/L^{3/2}$. The final positron, with momentum \vec{p}_e , will have a plane-wave wavefunction $\psi_e(\vec{x}) = e^{i\vec{p}_e\cdot\vec{x}/\hbar}/L^{3/2}$, and similarly the final neutrino and antineutrino will have wavefunctions $\psi_{\nu_e}(\vec{x}) = e^{i\vec{p}_{\nu}\cdot\vec{x}/\hbar}/L^{3/2}$ and $\psi_{\bar{\nu}_e}(\vec{x}) = e^{i\vec{p}_{\bar{\nu}}\cdot\vec{x}/\hbar}/L^{3/2}$, respectively.

Since the point-like weak interaction event can occur at any point in space, the complete amplitude will involve an integral over space with an integrand that is the product of the amplitude $\psi_{\mu}(\vec{x})$ to find the muon at some point \vec{x} , times the product of conjugate wavefunctions $\psi_e(\vec{x})^* \psi_{\nu_{\mu}}(\vec{x})^* \psi_{\bar{\nu}_e}(\vec{x})^*$, giving the amplitudes for the created positron, neutrino, and antineutrino all to be at (the same) point \vec{x} , all times some overall constant which will control the rate of this process,

$$M = \left[\int_{\mathcal{V}} d^3x \psi_e(\vec{x})^* \psi_{\nu_{\mu}}(\vec{x})^* \psi_{\bar{\nu}_e}(\vec{x})^* \psi_{\mu}(\vec{x}) \right] \times (\text{const.}). \quad (7.1.3)$$

For the weak interaction the overall constant is known as the *Fermi constant*, G_F , divided by $\sqrt{2}$. (Including this factor of $\sqrt{2}$ is merely a convention, but is required so that G_F matches its historical definition.) The integrand appearing in this matrix element is just a constant,

$$\psi_e(\vec{x})^* \psi_{\nu_{\mu}}(\vec{x})^* \psi_{\bar{\nu}_e}(\vec{x})^* \psi_{\mu}(\vec{x}) = \frac{e^{-i(\vec{p}_e + \vec{p}_{\nu} + \vec{p}_{\bar{\nu}})\cdot\vec{x}/\hbar}}{(L^{3/2})^4} = L^{-6}, \quad (7.1.4)$$

provided the momenta satisfy conservation of 3-momentum, $\vec{p}_e + \vec{p}_{\nu} + \vec{p}_{\bar{\nu}} = 0$.¹ Integrating over the region \mathcal{V} thus simply yields a factor of the volume, L^3 , of this region. Hence, we find

$$M = \frac{G_F/\sqrt{2}}{L^3}. \quad (7.1.5)$$

¹The mathematically astute will recognize that the integral over all (3 dimensional) space of an expression like the one in Eq. (7.1.4) produces precisely the Dirac delta function that ensures 3-momentum conservation, *i.e.*, translational invariance means integrating over all space means a delta function.

We noted above that the decay amplitude M must have dimensions of energy. Since $1/L^3$ has dimensions of energy cubed (having set $\hbar = c = 1$), we learn that the Fermi constant G_F must have dimensions of $1/(\text{energy})^2$.

The value of the Fermi constant G_F may be fixed by demanding that the muon decay rate Γ calculated from Eq. (7.1.2) agrees with the experimentally determined value. The decay rate is just the inverse of the lifetime, so $\Gamma = 1/\tau_\mu = 1/(2 \mu\text{s})$. Performing the sum over final states in Eq. (7.1.2) involves integrating over the final momenta subject to the constraints of energy and momentum conservation. Details of this calculation, which is straightforward, will be omitted. One finds that $\Gamma = G_F^2 m_\mu^5 / (192\pi^3)$. Note that the resulting natural units from $G_F^2 m_\mu^5 = \text{energy}^{-4} \text{energy}^5 = \text{energy} = \text{time}^{-1}$, just what we expect for a *rate* of decay. Equating this with the inverse of the experimentally measured decay rate and solving for G_F yields

$$G_F = 1.16637(1) \times 10^{-5} \text{ GeV}^{-2} \simeq 1.2 \times 10^{-5} \text{ GeV}^{-2} = 12 \text{ TeV}^{-2}. \quad (7.1.6)$$

7.2 Neutrino scattering

The significance of the determination of the Fermi constant described above comes from the fact that a factor of G_F will appear in *every* weak interaction amplitude. Consider, for example, the *inelastic* neutrino *scattering* process,

$$\nu_\mu + e^- \rightarrow \nu_e + \mu^-, \quad (7.2.1)$$

depicted on the left in Fig. 7.2 in which the “flavor” of the charged lepton changes. With sufficient experimental skill and resources, this is a measurable process. The cross section for this scattering process equals the rate of scattering events divided by the incident flux of neutrinos and the density of target electrons. For a neutrino beam with constant flux, the scattering rate is just the probability of scattering in time Δt , divided by Δt . And the probability, as always in quantum mechanics, is the absolute square of a probability amplitude which involves a matrix element of the weak interaction Hamiltonian between the relevant incoming and outgoing states, $M = \langle \text{out} | H_{\text{weak}} | \text{in} \rangle$. This weak interaction amplitude must also be proportional to G_F , so that²

$$\sigma \propto |M|^2 \propto G_F^2. \quad (7.2.2)$$

Now do some more dimensional analysis. A cross section is an area, with dimensions of length squared or (in natural units) $[\text{energy}]^{-2}$. The Fermi constant G_F also has dimensions of $[\text{energy}]^{-2}$, but G_F appears *squared* in the cross section. Therefore the cross section must equal G_F^2 times “something else” with dimensions of $[\text{energy}]^2$. What can this “something else” depend on? One possibility, which is surely relevant, is the neutrino energy. But the energy of a particle is frame-dependent. Since the cross section is an invariant concept (effectively the “size” *transverse* to the direction of the beam, which is not changed by boosts along the beam), we must be able to express the cross section in terms of Lorentz invariant quantities. A Lorentz invariant measure of the scattering energy is $s \equiv (p_{\nu_\mu} + p_e)^2 = (p_{\nu_e} + p_\mu)^2 = E_{\text{CM}}^2$. At low energies, the value of the cross section will also depend on the electron and muon masses. After all, if $E_{\text{CM}} < m_\mu c^2$, then the reaction $\nu_\mu + e^- \rightarrow \nu_e + \mu^-$

²In fact, analytic continuation in the four-momenta relates the amplitude for inelastic neutrino scattering, $\nu_\mu + e^- \rightarrow \nu_e + \mu^-$, to the amplitude for μ^+ decay. This relation, which involves replacing particles in the initial state by their antiparticles in the final state (or vice-versa) is known as *crossing symmetry*.

cannot possibly occur. So by “pure thought” we conclude that it must be possible to express the cross section in the (dimensionally consistent and invariant!) form

$$\sigma = G_F^2 s \times f\left(\frac{m_e}{\sqrt{s}}, \frac{m_\mu}{\sqrt{s}}\right), \quad (7.2.3)$$

where f is some *dimensionless* function of the *dimensionless* ratios m_e/E_{CM} and m_μ/E_{CM} . Further we expect (by energy-momentum conservation) that this function will be non-vanishing only when both arguments are less than one.

The simplest regime to consider is large energy relative to the muon mass, $E_{\text{CM}} \gg m_\mu c^2$. In this domain, the ratios m_e/E_{CM} and m_μ/E_{CM} are both tiny. Since the cross section can be expressed in the form (7.2.3), understanding the behavior of the cross section when the energy is large is the same problem as understanding the behavior of the cross section in a hypothetical world where the value of the electron and muon masses are arbitrarily small (compared to some reference mass scale).

A crucial observation is that there is no reason to expect anything dramatic, or singular, to happen in the limit of vanishingly small electron and muon mass (at fixed energy E_{CM}). In the relativistic relation between (total) energy and momentum, the zero mass limit is perfectly smooth, and just leads to the energy-momentum relation of a massless particle,³

$$E(\vec{p}) = \sqrt{\vec{p}^2 + m^2} = |\vec{p}| + \frac{1}{2} \frac{m^2}{|\vec{p}|} + \cdots \xrightarrow{m/E \rightarrow 0} |\vec{p}|. \quad (7.2.4)$$

Similarly, the massless limit of the function $f(\frac{m_e}{\sqrt{s}}, \frac{m_\mu}{\sqrt{s}})$ appearing in the cross section (7.2.3) should be expected to be finite and non-zero, so that $A \equiv f(0, 0)$ is just some pure number like 2 or π . A detailed calculation shows that, for the process (7.2.1), the number A is $1/\pi$. Therefore, the inelastic neutrino cross section is given by

$$\sigma_{\nu_\mu e^- \rightarrow \nu_e \mu^-} = \frac{G_F^2 E_{\text{CM}}^2}{\pi}, \quad (7.2.5)$$

when $E_{\text{CM}} \gg m_\mu c^2 (\gg m_e c^2)$. This quadratic rise of the cross section with center-of-mass energy (for energies above the relevant particle masses) also applies to other weak interaction scattering processes, including neutrino scattering with nucleons and elastic neutrino-electron scattering. In the latter example, the cross section is

$$\sigma_{\nu_e e^- \rightarrow \nu_e e^-} = 0.551 \frac{G_F^2 E_{\text{CM}}^2}{\pi}. \quad (7.2.6)$$

Recall, as we have already mentioned and will discuss in more detail in the next section, the weak interactions involve not only the exchange of the electrically charged W bosons (the so-called “charged current” weak interaction), as happens in the inelastic process of Eq. (7.2.5), but also the exchange of the electrically neutral Z boson (the so-called “neutral current” weak interaction), which contributes also to the elastic process in Eq. (7.2.6) (see the Feynman diagrams in Fig. 7.6). The differences in the two processes (one being only W exchange and the other both W and Z) leads to the different coefficient in Eq. (7.2.6) versus Eq. (7.2.5). The coefficient *decreases* by a factor of about 2 due to

³In contrast, the non-relativistic (kinetic) energy $E_{\text{NR}}(\vec{p}) = \vec{p}^2/(2m)$ is *not* well-behaved if $m \rightarrow 0$ for fixed momentum \vec{p} .

destructive interference between the W and Z exchanges (recall that quantum physics is all about interference).

For completeness we should also note the elastic cross section for the related (by crossing) process with antineutrinos,

$$\sigma_{\bar{\nu}_e e^- \rightarrow \bar{\nu}_e e^-} = 0.231 \frac{G_F^2 E_{\text{CM}}^2}{\pi}. \quad (7.2.7)$$

This cross section is smaller by approximately a factor of 3, which arises from the further fact (not present in our original simple point model) that the W (but not the Z) couples only to fermions of a definite spin projection. The W couples only to “left-handed” fermions (spin projection opposite the direction of motion) and “right-handed” antifermions (spin projection along the direction of motion). (Recall this is why the weak interactions violate both P , which transforms left-handed to right-handed, and C , which transforms particle to antiparticle.) In particular, this means that for the elastic neutrino-electron scattering process of Eq. (7.2.6) we have a left-handed neutrino scattering from a left-handed electron. Thus, viewed in the CM frame, the two spins are oppositely oriented and we have (total) $J_3 = 0$ for both the initial and final states. Thus angular momentum conservation imposes no constraints. In contrast, the anti-neutrino elastic scattering process of Eq. (7.2.7) involves a right-handed antineutrino scattering from a left-handed electron. Hence we have (total) $J_3 = 1$ along the direction of motion of the antineutrino in both the initial and final states. Hence “back”-scattering of the antineutrino (and the electron) is not allowed by angular momentum conservation, since it would require turning $J_3 = +1$ into $J_3 = -1$. In fact, compared to the neutrino process, the scattering cross section of the antineutrino process is reduced at all scattering angles except exactly forward ($\theta = 0$). Thus the “handedness” in the weak dynamics explains both why the weak interactions do not respect parity and the extra factor of about 1/3 in Eq. (7.2.7).

These predictions of neutrino cross sections increasing with increasing energy, which arise directly from our simple picture of the weak interactions as a point interaction, have been confirmed experimentally for energies in the multi-MeV to multi-GeV range.⁴ But the prediction of quadratically rising cross sections raises an immediate puzzle: can cross sections really grow with increasing energy *forever*? Or is there some point at which the behavior must change?

In fact, cross sections *cannot* become arbitrarily large. The number of scattering events in any scattering experiment is proportional to the cross section. But ultimately, the number of scatterings cannot be larger than the total number of projectiles! A quantum mechanical analysis shows that for point-like (or so-called s -wave) scattering, the cross-section must satisfy the bound

$$\sigma < \frac{\lambda^2}{4\pi} = \frac{\pi}{p^2}, \quad (7.2.8)$$

where $\lambda = 2\pi\hbar/|\vec{p}|$ is the de Broglie wavelength of the projectile in the center-of-mass frame. This is referred to as a *unitarity* bound.

For an ultra-relativistic scattering, viewed in the center-of-mass frame, the energy of each particle is almost the same as the magnitude of its momentum (times c), and hence $E_{\text{CM}} \simeq 2|\vec{p}|$. Equating expression (7.2.5) for the neutrino cross section with the unitarity bound (7.2.8), one finds that the

⁴See, for example, the plots of the (anti)neutrino-nucleon total cross section at the particle data group website (see page 9). Note that for neutrino scattering on a nucleus, the lab frame energy is proportional to the square of the center-of-mass energy, $E_{\text{lab}} \propto E_{\text{CM}}^2$, when E_{lab} is large compared to the target mass. So the quadratic rise of the cross section with E_{CM} is equivalent to linear growth as a function of E_{lab} , and a *constant* behavior for σ/E_{lab} , as plotted.

cross section (7.2.5) violates the unitarity bound when the center-of-mass energy exceeds

$$E^* \equiv \sqrt{\frac{2\pi}{G_F}} \approx 700 \text{ GeV}. \quad (7.2.9)$$

Therefore, at some energy below 700 GeV, something must dramatically change the behavior of weak interaction cross sections to stop their quadratic rise with increasing energy. In fact, before we reach this energy the weak interactions begin to exhibit the fact that they do not really correspond to a *point* interaction, but rather to the exchange of the aforementioned W 's and Z 's.

7.3 Weak gauge bosons

At energies somewhat below E^* , weak interaction cross sections become comparable to electromagnetic cross sections. At this point, one might anticipate significant changes in the behavior of both electromagnetic and weak interactions. This turns out to be true. Figure 7.4 shows the cross section for electron-positron annihilation into hadrons as a function of $\sqrt{s} = E_{\text{CM}}$. At energies below about 50 GeV, one sees that the cross section generally decreases with increasing energy (note the logarithmic scale). Since the electromagnetic coupling is dimensionless (unlike the weak interactions, there is no symmetric breaking for EM and no mass scale), the same dimensional analysis we applied to the weak interactions yields electromagnetic cross sections that behave like α^2/s (instead of $G_F^2 s$) and this is the general fall-off we see in the upper plot in Figure 7.4. The lower plot in Figure 7.4 shows the *ratio* between $e^+e^- \rightarrow \text{hadrons}$ and $e^+e^- \rightarrow \mu^+\mu^-$, which cancels out the $1/s$ behavior. In fact, the levels of the various “flat” sections in this plot are easily understood in terms of *sum* over the squares of the electric charges of the quarks to which the photon couples, with the scale of the charge e^2 canceled out by the charge (squared) of the muon in the denominator. Thus at low energies, where only u, d, s quarks are produced, the ratio is

$$\begin{aligned} R_{\text{low}} &= 3 \left[\left(\frac{2}{3} \right)^2 + \left(\frac{-1}{3} \right)^2 + \left(\frac{-1}{3} \right)^2 \right] \\ &= 3 \left[\frac{4}{9} + \frac{1}{9} + \frac{1}{9} \right] = 2. \end{aligned} \quad (7.3.1)$$

In this expression the preceding factor of 3 accounts for the fact that quarks come in 3 colors, which contribute equally to the coupling to photons but are distinct and do not interfere (*i.e.*, you square the amplitude for each color *first* and *then* sum over colors). As the energy increases, quarks with larger masses contribute and the value of R takes a step up at each threshold (to produce a new flavor pair). At the c quark threshold (where we also see the $c\bar{c}$ bound state resonances J/ψ and $\psi(2S)$) we add an additional $3 \times 4/9$ and R increases to $10/3$. At the b quark threshold (marked by the $b\bar{b}$ Υ resonance) R is increased by $3 \times 1/9$ to $11/3$. The fact that this simple picture of quarks with the specified (if peculiar) fractional electric charges and in 3 colors is in such good agreement with the data was an essential step in the general acceptance of the current Standard Model of particle physics.

The other dramatic feature of Figure 7.4 is the appearance of the various spin one, parity odd hadronic resonances — the broad ρ and ρ' , the narrower ω and ϕ , and the very narrow “spikes” associated with $c\bar{c}$ and $b\bar{b}$ heavy quark states (already mentioned above). The J/ψ and $\psi(2s)$ are $c\bar{c}$ bound states with energies close to twice the charm quark mass, while the upsilon (Υ) states near

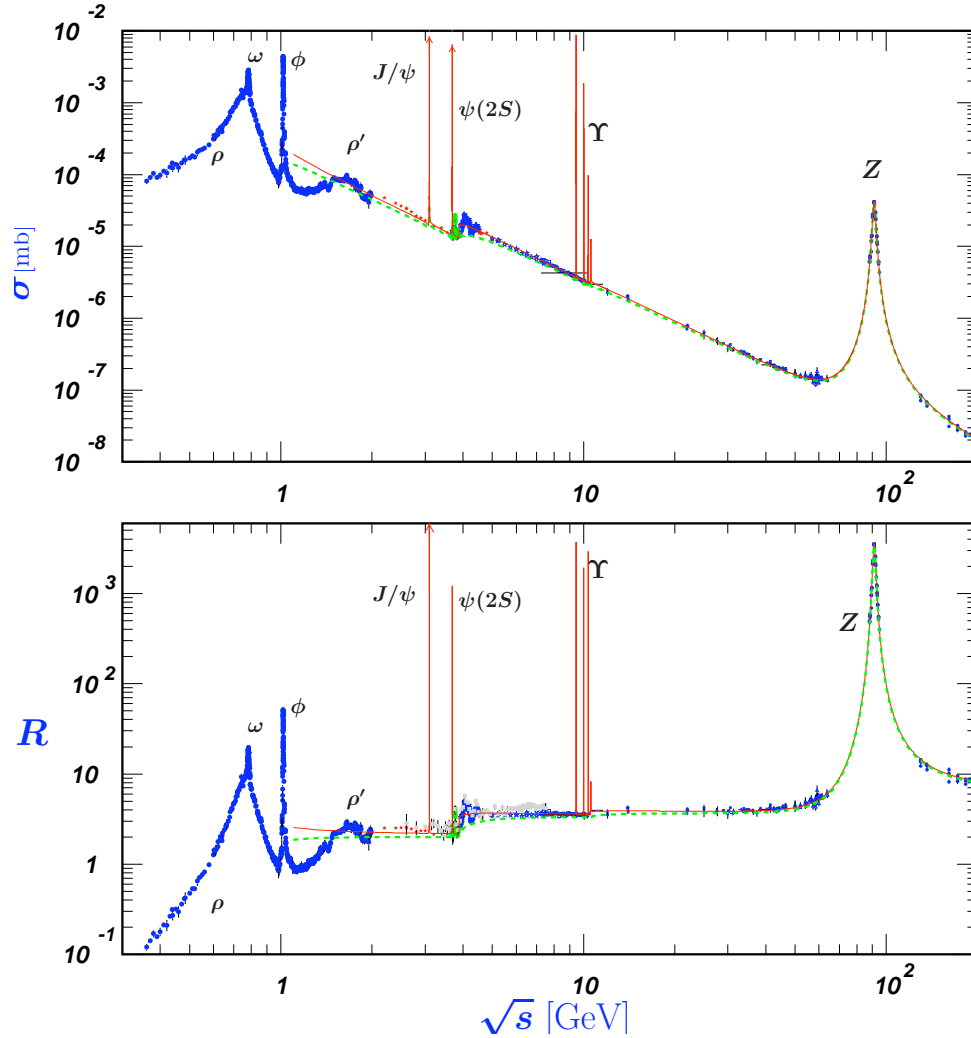


Figure 7.4: Top: Cross section for e^+e^- annihilation to hadrons as a function of $\sqrt{s} = E_{\text{c.m.}}$. Bottom: Ratio of cross sections for e^+e^- annihilation to hadrons versus annihilation to muon pairs, $R = \sigma_{e^+e^- \rightarrow \text{hadrons}} / \sigma_{e^+e^- \rightarrow \mu^+\mu^-}$. particle data group website (see page 6).]

$2m_b$ are $b\bar{b}$ states. But then, at a much higher energy near 90 GeV, there is a very large resonance which is something new and relevant to our current discussion. This is not a quark-antiquark bound state, but rather a new type of particle which is called the Z boson. The same resonance appears in neutrino scattering. There is also a closely related pair of charged particles known as the W^+ and W^- . These are not seen in Figure 7.4 because a single W^+ or W^- cannot result from e^+e^- annihilation — this would violate charge conservation! However, the W bosons are present in those interactions where a quark or lepton changes type (*i.e.*, flavor) and they can be pair ($W^+ + W^-$) produced in $e^+ + e^-$ annihilation at energies above $2M_W c^2$, *i.e.*, off the above plot to the right..

Together, the W^\pm and Z are known as *weak gauge bosons*.⁵ They are spin one particles with masses

⁵The word “gauge” appears here because the underlying (broken) $SU(2)$ symmetry is of a type called a “gauge

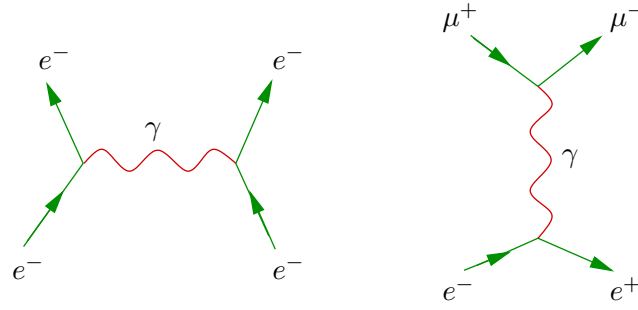


Figure 7.5: Feynman diagrams for Coulomb scattering: $e^-e^- \rightarrow e^-e^-$ (left), and electron-positron annihilation to muons: $e^+e^- \rightarrow \mu^+\mu^-$ (right).

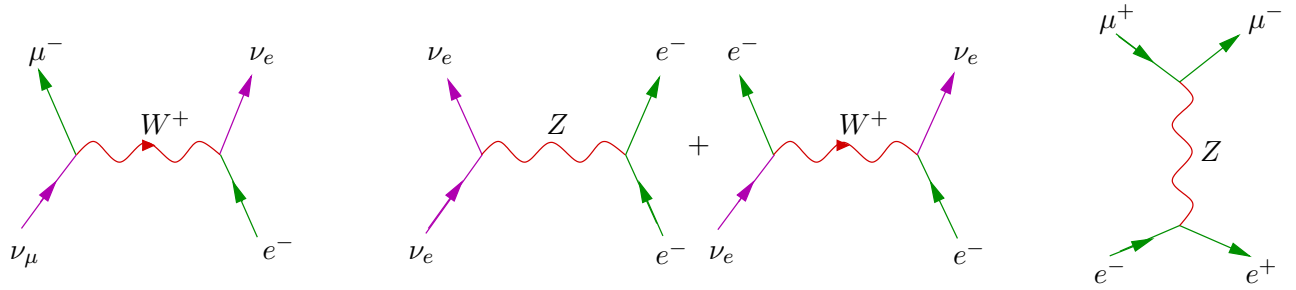


Figure 7.6: Feynman diagrams for inelastic neutrino scattering: $\nu_\mu + e^- \rightarrow \nu_e + \mu^-$ (left), elastic neutrino scattering: $\nu_e + e^- \rightarrow \nu_e + e^-$ (middle), and the weak interaction contribution to $e^+e^- \rightarrow \mu^+\mu^-$ (right).

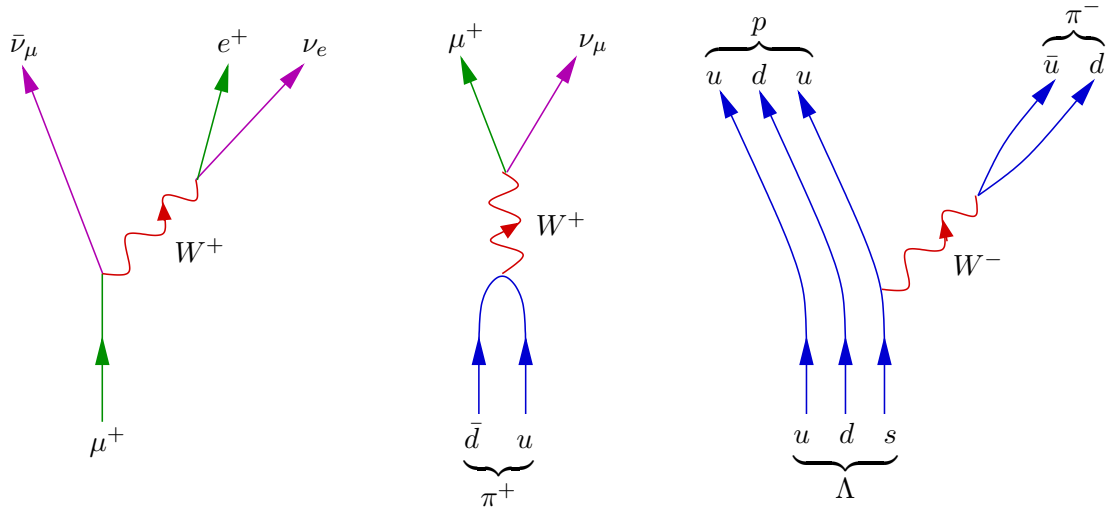


Figure 7.7: Depictions of the weak decays $\mu^+ \rightarrow e^+ + \bar{\nu}_\mu + \nu_e$ (left), $\pi^+ \rightarrow \mu^+ + \nu_\mu$ (middle), and $\Lambda \rightarrow p + \pi^-$ (right), showing the exchange of weak gauge bosons.

$$m_W = 80.385 \pm 0.015 \text{ GeV}, \quad m_Z = 91.1876 \pm 0.0021 \text{ GeV}. \quad (7.3.2)$$

The simplest current picture is that these masses for the weak gauge bosons arise from the interaction between the weak gauge bosons and the (apparently now found) Higgs boson, which itself is assumed to have a nonzero “vacuum expectation value” or $\langle 0|h|0 \rangle \neq 0$. (The data from the LHC suggest pretty clearly that a Higgs boson with the expected properties and a mass of about $125 \text{ GeV}/c^2$ has been detected.) The weak gauge bosons mediate the weak interactions, in the same sense that the photon is responsible for mediating electromagnetic interactions. Coulomb interactions may be viewed as resulting from the exchange of photons between charged particles, and a process like $e^+e^- \rightarrow \mu^+\mu^-$ may be regarded as occurring via the annihilation of the electron and positron into a (virtual) photon, which lives only a very short time before converting into the final μ^+ and μ^- . The diagrams of Figure 7.5 depict these electromagnetic processes.

In the same fashion, weak interactions may be regarded as arising from the exchange of W and Z bosons. Figure 7.6 depicts the same weak interaction scattering processes illustrated in Figure 7.2, plus the weak interaction contribution to $e^+e^- \rightarrow \mu^+\mu^-$, explicitly showing the exchange of weak gauge bosons. Figure 7.7 does the same for the weak decays of Figure 7.1. These diagrams illustrate the fact that the (lowest order) weak interactions are not really “point” interactions, but rather localized to a small, but nonzero scale of order $1/M_W \sim 2 \times 10^{-3}$ fermi. For particles with de Broglie wavelengths short enough to probe this sort of distance (*i.e.*, $E \gg 100 \text{ GeV}$), the character of the weak interactions is moderated and the cross section stops increasing quadratically with the (CM) energy (and eventually decreases as $1/E_{\text{CM}}^2$). Note also that it is the difference between the left-hand diagram and the middle diagram in Figure 7.6 that explains the difference between the cross sections in Eqs. (7.2.6) and (7.2.5).

The diagrams of Figures 7.5–7.6 are examples of *Feynman diagrams*. They actually do more than merely depict some process — these diagrams encode precise rules for how to calculate the quantum mechanical amplitude associated with each process. But developing this in detail (*e.g.*, in QFT) will have to be left for a subsequent class.

With this brief sketch of the current understanding of weak interactions, we must conclude our introduction to particles and symmetries. Hopefully it has whetted your appetite to learn more about this subject.

symmetry”.